Chemical Science

ROYAL SOCIETY OF CHEMISTRY

MINIREVIEW

View Article Online
View Journal | View Issue

Cite this: *Chem. Sci.*, 2020, **11**, 6642

All publication charges for this article have been paid for by the Royal Society of Chemistry

Received 3rd May 2020
Accepted 15th June 2020

DOI: 10.1039/d0sc02507k

rsc.li/chemical-science

Noble gas endohedral fullerenes

Said Jalife, †*[a] Jessica Arcudia, [a] Sudip Pan *[b] and Gabriel Merino *[a]

This review focuses on the available experimental and theoretical investigations on noble gas (Ng) endohedral fullerenes, addressing essential questions related to the mutual effects that confinement of one or more Ng atoms induces on the electronic structure, bonding, and different properties of fullerenes. It also summarizes the different contributions to the mechanisms of formation and decomplexation, the reactivity towards Diels–Alder cycloaddition reactions, the chemical bonding situation of Ng endohedral fullerenes, and the interactions that dominate within these systems.

Evidence and preparation

Since the discovery of buckminsterfullerene (C_{60}) by Kroto, Smalley, and co-workers,[1] one of the most intriguing features that fascinates researchers is its hollow interior, large enough to enclose atoms and molecules. Sprang *et al.*[2] reported early works on the existence of endohedral fullerenes, incorporating metal atoms during the preparation of fullerenes using graphite, as in the well-known case of La@C_{60}.[3,4] Over time, the list of metallofullerenes (*e.g.*, Sc@C_{60}, Sc_2@C_{60}, Sc_3@C_{60}) has been gradually increased[5] and more than half of the elements have now been confined within fullerenes.[6–8] Perhaps, one of the groups that has attracted the most attention is the non-metal endohedral fullerenes, particularly those containing one or multiple noble gas (Ng) atoms, see Fig. 1. These endohedral fullerenes have been considered extremely stable complexes from the kinetical point of view. Some of the questions that have driven investigations of these systems are: to what extent the properties of fullerenes are affected by the encapsulation of Ng atoms? What kinds of interactions dominate within these systems? Can an Ng atom form a chemical bond with a cage atom and/or with another Ng atom in a confined state? How can Ng be inserted into fullerenes?

The first evidence of endohedral fullerenes containing Ng atoms came from the group of Schwarz[9–11] in a series of high-energy collision experiments. It was simultaneously described that the collision of He and Ne with positively charged C_{60}^{q+} (q = 1, 2, 3) entities led to the addition of the Ng mass to the ions.[9–21] Although neutralization–reionization experiments supported the helium (He) encapsulation,[11] it was indubitably not possible to know if the ions still retained their fullerene form. However, since the 1990s, different methods have been developed to encapsulate Ng atoms within fullerenes. Saunders *et al.*[22] detected He@C_{60} and Ne@C_{60} (at the part per million level) following the standard method of preparing fullerenes, *i.e.*, heating a graphite arc at 600 °C in the partial pressure of helium or neon. Subsequently, Saunders *et al.*[23] incorporated argon (Ar), krypton (Kr), and xenon (Xe) into fullerenes (Ar@C_{60}, Kr@C_{60}, Xe@C_{60}) by employing high temperature and pressure on a mixture of fullerenes and the target Ng. It was proposed that the encapsulation process occurs through the "window mechanism", where a temporary window gets formed by breaking one or more C–C bonds within the cage. Other techniques used to include Ng atoms into fullerenes are bombarding fullerenes with accelerated ions[24] or *via* the explosive method,[25] where a deliberate explosion in a mixture of Ng atoms and fullerene in a closed place led to the desired inclusion product (for He@C_{60} and He_2@C_{60}). Furthermore, a higher encapsulation ratio (30%) can be achieved using the so-called "molecular surgery" methodology,[26] which involves an opening of the cage, then the insertion of an atom, and finally the closure of the cage as reported for He@C_{60} and He@C_{70} systems (see Fig. 2 for an example that proceeds *via* an opening of a 13-membered ring).[26,27]

The properties and reactivity of endohedral fullerenes containing Ng atoms have been assessed mostly by ^{3}He NMR spectroscopy. Surprisingly, Saunders *et al.*[28] reported the chemical shift of helium at −6.36 ppm for ^{3}He@C_{60} and −28.81 ppm for ^{3}He@C_{70} relative to the resonance of free ^{3}He dissolved in 1-methylnaphthalene.[28,29] The observed ^{3}He shifts were rationalized in terms of a diamagnetic aromatic ring current in C_{60} and C_{70} with higher intensity owing to the diamagnetic nature of the benzenoid rings.[30] Therefore, an upfield in ^{3}He shift reflects a diatropic ring current (aromaticity), and a downfield shift means a paratropic ring current (antiaromaticity). This idea was pushed to the limit for the hexaanions He@C_{60}^{6-} (most shielded) and He@C_{70}^{6-} (most

[a]*Departamento de Física Aplicada, Centro de Investigación y de Estudios Avanzados, Antigua carretera a Progreso Km 6, Cordemex, Loma Bonita Xcumpich, 97310 Mérida, Yucatán, Mexico. E-mail: said.jalife@cinvestav.mx; said.jalifejacobo@chem.ox.ac.uk; gmerino@cinvestav.mx*

[b]*Fachbereich Chemie, Philipps-Universität Marburg, Hans-Meerwein-Straße, 35032 Marburg, Germany. E-mail: pans@chemie.uni-marburg.de*

† Current address: Chemistry Research Laboratory, 12 Mansfield Road, Oxford, UK.

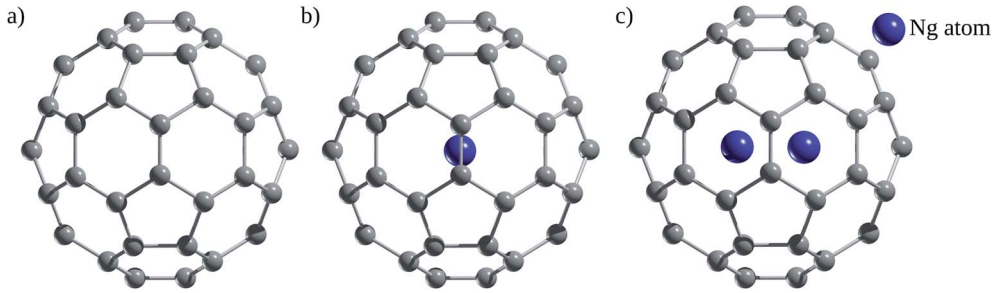

Fig. 1 (a) Free C_{60} and endohedral (b) Ng@C_{60} and (c) Ng_2@C_{60}.

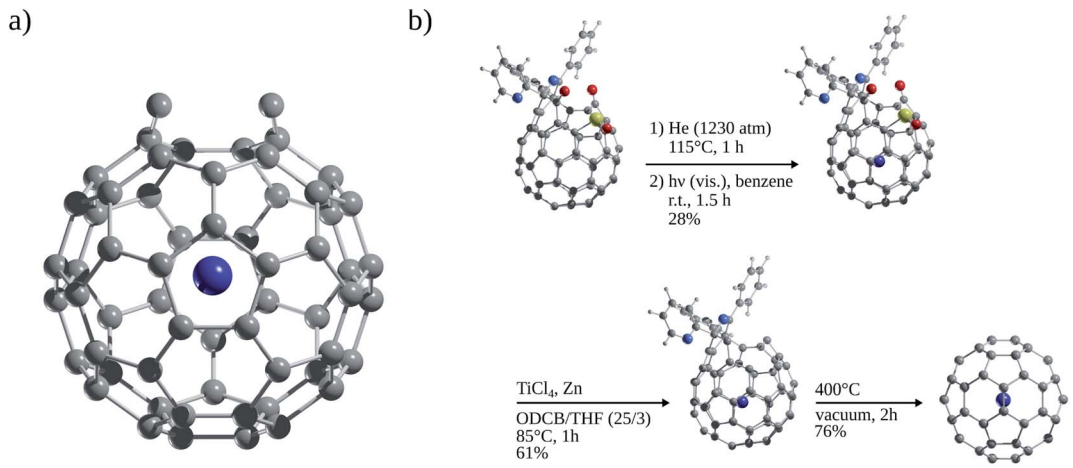

Fig. 2 (a) C_{60} with an open window and (b) encapsulating Ng atom by molecular surgery in C_{60}.

deshielded) compounds (^{3}He chemical shifts of −49.27 and +8.20 ppm, relative to ^{3}He in THF-d_8, respectively).[29,30] These values mean an opposite magnetic behavior compared to their neutral analogues and a significant change in the internal magnetic field and aromatic character, *i.e.*, He@C_{60}^{6-} is, in principle, more aromatic than the parent neutral compound. In further studies, the shielding of the encapsulated ^{3}He core in He@C_{60}^{6-} was rationalized by the presence of a long-range shielding cone along the entire cage due to its spherical aromatic character, whereas He@C_{70}^{6-} exhibits a strong deshielding response inside the cage to the induced magnetic field.[31,32] Also, the ^{3}He shielding was assessed in terms of the number of addends in arylated and cloro[60]fullerenes.[33] Based on the ^{3}He upfield shift, Birkett *et al.*[33] noted an enhanced aromatic character for all the aryl and chlorine C_{60} derivatives ($C_{60}Cl_6$–δ_{He} = −12.30 ppm, $C_{60}Ph_5Cl$–δ_{He} = −15.14 ppm, C_{60}(4-$FC_6H_4)_5Cl$–δ_{He} = −15.04 ppm, C_{60}(4-$FC_6H_4)_5^+$–δ_{He} = −12.61 ppm and 1,4-$C_{60}Ph_2$–δ_{He} = −10.50 ppm, $C_{60}Ph_4$–δ_{He} = −14.40 ppm) relative to the parent compound due to the introduction of an sp^3-hybridised carbon in adjacent pentagonal rings and an improved electronic delocalization in adjacent hexagons. This is associated with the high electronegativity of Cl atom, which reduces the *p*-character of adjacent carbons, and so the electron delocalisation. A similar assessment was performed with the bis- to hexakisadducts of C_{60} and mono- to tetrakisadducts of C_{70}.[34] For the C_{60} series, ^{3}He chemical shift decreases as a function of the degree of functionalization (from −8.11 to −11.89 ppm), whereas in the C_{70} series, ^{3}He chemical shift increases (from −27.53 to −20.68 ppm). While this contrasting behavior in C_{60} is attributed to the balance between paramagnetic pentagonal ring currents and diamagnetic benzenoid ring currents,[28] the upfield in C_{70} is explained by the interruption of the diamagnetic ring current along the corannulene perimeter.

Now, what is the influence of the encapsulated Ng atoms on the ^{13}C chemical shifts for the C_{60} cage? Murata and co-workers[27] reported the ^{13}C NMR spectra for free C_{70} and He@C_{70}. The He@C_{70} spectrum is quite similar to that of C_{70} (δ = 150.91, 148.36, 147.67, 145.64, 131.15 ppm) with only two slight signals shifted by less than 0.05 ppm within the sp^2 carbon region (145.66 and 131.15 ppm), revealing that He is located almost at the cage centre. More pronounced downfield shifts of 0.17, 0.39 and 0.95 ppm are observed in Ar@C_{60},[35] Kr@C_{60},[36] and Xe@C_{60},[37] respectively.

Single-crystal X-ray analysis also provided clear evidence on the structure of Ng atoms inside fullerenes. Morinaka *et al.*[38] crystallized He@C_{60}·{Ni^{II}(OEP)}$_2$ (see Fig. 3a), confirming that He is at the centre of the C_{60} with 100% of occupation level. Dragoe and co-workers[39] described the extended X-ray absorption fine structure for Kr@C_{60}, while Balch and co-workers[40] reported the crystal structure of Kr@C_{60} in (0.09Kr@C_{60}/0.91C_{60})·{Ni^{II}(OEP)}$_2C_6H_6$ (Fig. 3b). In the case of Ar@C_{60}, the endohedral nature of Ar was confirmed by X-ray photoelectron

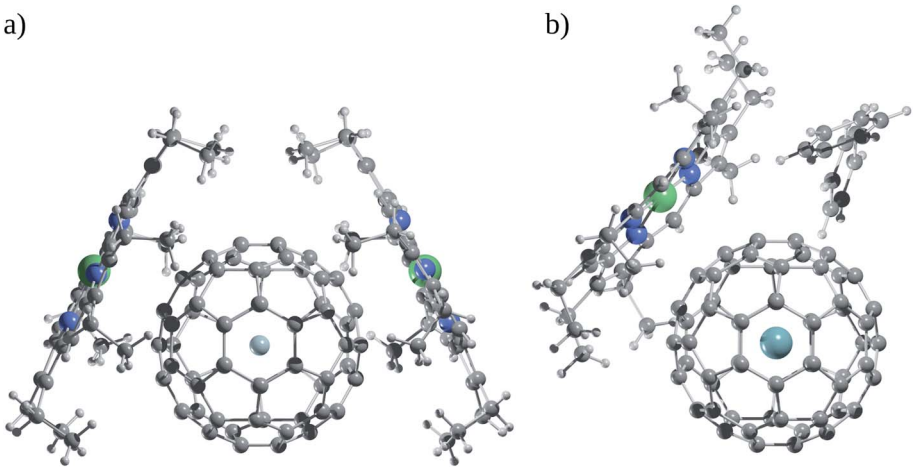

Fig. 3 (a) X-ray structures of $He@C_{60}\cdot\{Ni^{II}(OEP)\}_2$ and (b) $(0.09Kr@C_{60}/0.91C_{60})\cdot\{Ni^{II}(OEP)\}\cdot 2C_6H_6$.

spectroscopy and photoelectron diffraction,[41] as well as by extended X-ray absorption fine structure experiments.

Encapsulation and release process of Ng atoms

From high-pressure experiments, Saunders *et al.*[22] estimated an Arrhenius activation energy of ~80 kcal mol^{-1} for the release of He from fullerene. In contrast, the computed activation barrier for He insertion into C_{60} through a six-membered ring is >200 kcal mol^{-1}.[14,19,42–44] Therefore, the release mechanism does not follow the penetration route. From mass spectroscopic studies, it is apparent that the Ne atom is released without destroying the C_{60} cage.[45] This evidence suggests that Ng release occurs through a window mechanism or molecular surgery, in which C–C bonds are broken to open the cage, the inner Ng is released, and then the cage is reconstituted. In the case of the Kr and Xe derivatives, barriers are even higher than 1500 kcal mol^{-1} for inserting Ng through a six-membered ring of C_{60}.[46] Other processes involving the formation of triplet states were considered but they require even higher activation energies. Moreover, the incorporation fractions of ^{3}He and ^{4}He increase in the presence of cyanide (KCN),[47] suggesting that the insertion of Ng may involve more than two species.

To obtain a better understanding of the dynamics of encapsulation and release of Ng within fullerenes, several molecular dynamics (MD) simulations and quantum chemical computations were carried out. Some of the first works employed classical MD to study the formation process of $Ng@C_{60}$ endohedral fullerenes. Cui *et al.*[48] reported the formation process of $Ng@C_{60}$ (Ng = He–Kr) endohedral fullerenes by a collision of Ng atoms with C_{60} using classical MD with a Tersoff and Lennard-Jones potentials to model all the C–C and Ng–C interactions, respectively. Three mechanisms of formation emerged: ring insertion, windowing, and holes. The first one is the insertion of an Ng into the C_{60} cage through a pentagon or hexagon ring without breaking any C–C bond, the second involves the formation of a short window when a C–C bond is broken due to the transfer of kinetic energy from the incident atom, while in the hole mechanism the same occurs, but the Ng is trapped within a defected C_{60} cage. $He@C_{60}$ and $Ne@C_{60}$ could be formed *via* ring-insertion or windowing mechanisms. Xu *et al.*[49] investigated the complexation and decomplexation process of $He@C_{60}$ using quantum chemical computations. Four possible paths were explored: insertion of He through the centre of a five-membered ring, through a six-membered ring, and through the centre of the [6,6] or [5,6] C–C bonds. In all the cases, a planar and spherical expansion was considered. The computed barriers support the increase of the [5,6] bond lengths, forming a 9-membered ring window as the most probable path (~250 kcal mol^{-1}), whereas the other options involve barriers above 300 kcal mol^{-1}. So, the insertion of He into C_{60} is easier *via* the expansion of a plane window than a spherical window.

Zahn *et al.*[50] studied the effect of pressure incorporating He into C_{60} using combined quantum/classical molecular dynamics QM/MM/MD simulations, particularly a path-sampling algorithm. The simulations included 1000 He atoms and a C_{60} molecule at 50 atm and 1000 K. The analysis of insertion trajectories reveals that the He incorporation occurs through a window formed by the opening of three C–C bonds. The lifetime of the opening is in the range of 50 to 150 fs, and the insertion of He requires around 120 kcal mol^{-1}. Previously, Patchkovskii *et al.*[42] computed (at the MNDO, HF/3-21G, and BP86/3-21G levels) the barriers of He incorporation into C_{60} through the opening of one-bond and two-bond windows. However, the barriers (>200 kcal mol^{-1}) are further away from the experimentally reported ones (~80 kcal mol^{-1}).

The radical impurity insertion mechanism for $C_{60}X$ and $C_{60}X_2$ (X = H and Me) systems using semiempirical MNDO and density functional theory (DFT) computations (BLYP/3-21G) was also screened by Patchkovskii *et al.*[51] Sixty-five different pathways for the insertion of He through six-membered rings and different windows in $C_{60}X$ and $C_{60}X_2$ were reported. Although the barriers are much lower compared to C_{60} when an impurity is added (*i.e.* $C_{60}X$ and $C_{60}X_2$), the computed values were very high compared to the experimental ones.

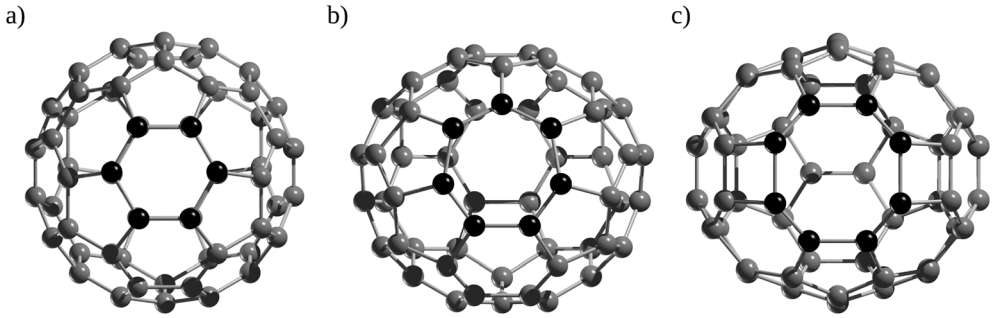

Fig. 4 Atomic structure of (a) C_6 on C_{60}, and (b) C_7, (c) C_8 on C_{58}, respectively.

Roth and co-workers[52] studied the effect of the Ng encapsulation on C_{60} at higher temperatures (T = 160–1500 K) using a Lennard-Jones potential for the Ng–C interactions along with a Brenner's empirical extended bond-order potential for the C–C bonds. These simulations show that smaller Ng atoms sit more off-centre than large ones and that the cage can be stabilized or not by stifling radial fluctuations. Similar MD simulations at higher temperatures (T = 4000–5000 K) indicate that the rate of release of Ng atoms does not only depend on the size of the Ng, but also because heavier encapsulated Ng atoms tend to stabilize the cage against thermal fluctuations.[53] However, there is no evidence of a closing mechanism of the cage after the escape of Ng through a formed window. The same group[54] also simulated an aggregate formed by five Ne@C_{60} endohedral molecules at temperatures ranging from T = 1000 K to T = 5000 K. The aggregate dissociates at 1150 K, but the carbon cages remain intact up to 4000 K, in which the Ne atom releases the aggregate through a window that opens and closes, but which remains as a defect at about 5000 K. Nevertheless, based on the experiments, it was suggested the limitation of classical dynamics to describe these systems at temperatures below 3000 K.

Ab initio MD simulations were also employed to investigate the formation process of He@C_{60} by simulating the explosion method (*vide supra*). Peng and co-workers[55] used *ab initio* MD simulations at the PBE-vdw/DZP level to characterize the reaction path for colliding He into C_{60} and the formation process of He@C_{60}. Initially, the authors computed a barrier of around 225 kcal mol^{-1} to insert He through a six-membered ring. However, the defects formed on fullerene are able to decrease this barrier. For instance, when a C_2 unit is removed to form a C_{58} cage, considering a Rice shrink-wrap mechanism known in C_{60}, He insertion can take place through a C_7 or C_8 rings (Fig. 4b and c) with approximate barriers of 123.6 and

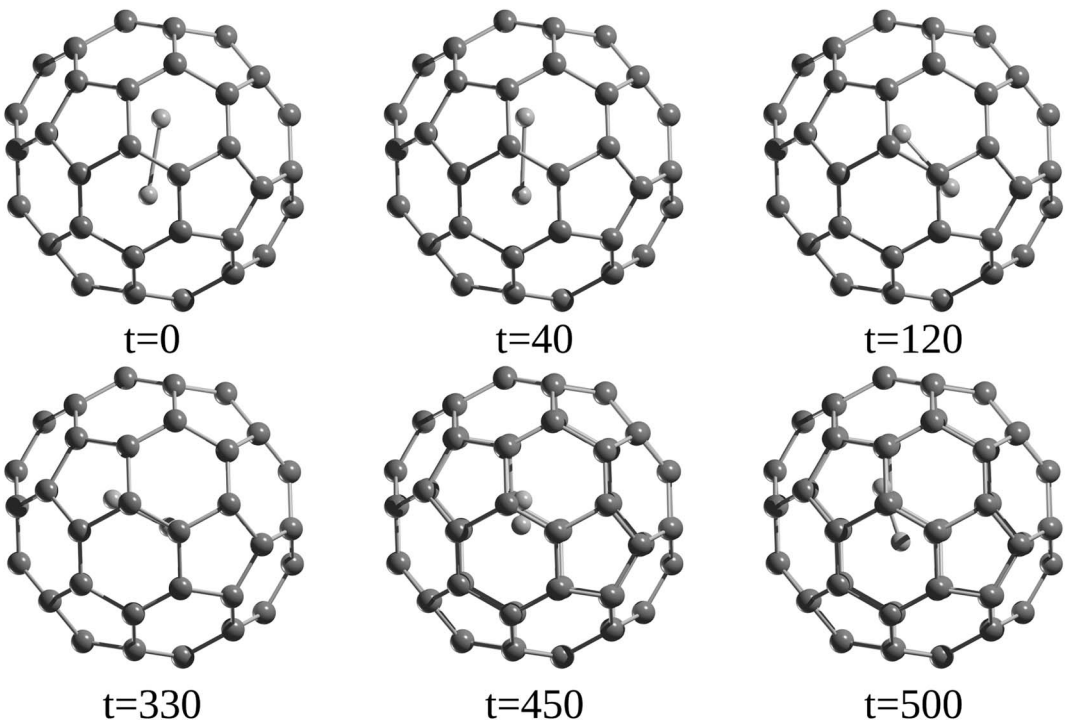

Fig. 5 Snapshots at different time steps of He_2@C_{60} system. Time in fs.

70.0 kcal mol^{-1}, respectively, or even better, when a collision between two C_{60} is simulated, the insertion barrier can decrease to 60.0 kcal mol^{-1} through a C_9 ring. In fact, it was reported by tandem mass spectrometry studies that C_{70}^+, Ne@C_{70}^+, and Ar@C_{70}^+ cations undergo cage-shrinking reactions by unimolecular elimination of a C_2 unit, which has lower activation energies than the removal of endohedral Ng atoms.[56]

A detailed analysis of the dynamics of encapsulated Ng atoms was carried out by Li *et al.*[55] and Khatua *et al.*,[57] showing that for Ng atoms in the Ng_2@C_{60} (Ng = He–Kr) family, a nearly free precession movement around its midpoint in the C_{60} cage is possible, which depends on two factors, the interaction between the Ng and the cage and the distortion of the cage caused by the precession movement (see Fig. 5). DFT computations also predicted such behavior for the internal rotation of Ng atoms inside the C_{70} cage. According to Gómez *et al.*,[58] the encapsulated Ng_2 dimer within a C_{70} cage can rotate as well, and He_2 rotates more readily than its heavier analogues Ne_2 and Ar_2.

The effect of confinement on chemical bonding

The completely filled valence shell of Ng atoms, their reasonably high ionization energies, and low electron affinities make them very lazy species to form chemical bonds with other elements. A really strong polarizing centre is required to deform the rigid electron density of Ng and to attract towards itself, facilitating a donor–acceptor type of interaction. Gold[59] and beryllium,[60–63] with the appropriate combination of geometrical orientation and charge distribution, make them the best transition metal and main-group elements, respectively, to form such type of interaction. Another strategy of forming a strong bond involving Ng is to push it in an extreme situation and to make the charge distribution in a way that this atom acts as cation Ng^+ and then providing enough kinetic stability, at least, up to certain temperatures. Metastable Ng insertion complex, XNgY is one of such examples where Ng is inserted into the X–Y bond, sacrificing its strength, and the resulting charge distribution should be $(XNg)^+Y^-$, where X–Ng bond is a strong electron-sharing bond.[64] But such molecules are thermochemically unstable with respect to dissociation, XNgY → Ng + XY. Another extreme situation is Ng endohedral complexes, where Ng atoms are forced to stay within a small space. Given the many bonds should be broken to be released from the cage, once one affords high energy to get it, the resulting Ng encapsulated complexes would be kinetically stable at ambient even at elevated temperatures. It provides a huge scope to force Ng atoms towards forming chemical bonds not only with the host atoms but also between two Ng atoms, which is otherwise unbound in nature, only weakly supported by tiny van der Waals forces. Given the fact that the chemical bond is a fuzzy concept (not an observable), these Ng inclusion complexes also draw arguments and counter ones regarding the existence of a chemical bond involving Ng atoms.

One aspect is the energetics. Several authors reported the interaction or complexation energies of Ng@C_n systems[65–78] (Ng = He–Xe; n = 20–60) using the Lennard-Jones model, or DFT and *ab initio* methods taking into account the dispersion effects and the basis set superposition error (BSSE). The general trend is that if the cavity size is small, lighter Ng atoms have more favorable interaction energies than their heavier analogues, but if the cage size is reasonably large, the heavier Ng atoms interact more strongly than the lighter ones. This is because the overall interaction energy depends on a delicate balance between attractive forces, originated from orbital, coulombic, and dispersion interaction, which increases linearly from lighter to heavier Ng atoms, and the Pauli repulsion that also enhances along the same direction. For instance, Bühl *et al.*[77] reported, at the counterpoise-corrected MP2/6-31G** level (using a DZP basis for Kr and Xe), negative interaction energies between endohedral He to Xe atoms and C_{60} of −0.3 (−2.0 at the MP2/TZP(C) + cc-pVQZ),[76] −1.9, −2.5, −7.5, and −5.4 kcal mol^{-1}, respectively, whereas GGA BLYP[79,80] and BP86 functionals,[79,81] and hybrid B3LYP[82] functional predict positive values (with BSSE). In the cases of hybrid GGA dispersion corrected B3LYP-DCP,[83] the empirically dispersion corrected B97-D,[84] and the hybrid meta-GGA functional M06-2X,[85] negative interaction energies (with BSSE) are obtained. Sure *et al.*[86] also nicely showed that the inclusion of dispersion contributions[87] in the Ng@C_{20+2n} (n = 0, 2–20; Ng = He, Ne, Ar) systems is mandatory in order to get reliable interaction energies. BP86-D/TZVPP level, with further energy refinement at the *ab initio* MP2/TZVPP level, was also found to be suitable to detail structures and energetics of Ng encapsulated C_{60} complexes correctly.[88] The BP86 functional combined with dispersion correction (D3 or D3(BJ)) can also describe such systems.[89] Therefore, in general, any functional that takes into account short-range and/or long-range dispersion interactions or *ab initio* methods in combination with sufficiently large basis set would provide reliable energetics.[71,86,90,91]

Now, does confinement induce a chemical bond? Since confinement pushes the bonding in extreme situations under high pressure, many models of bonding are bound to fail to explain them, starting a debate. Helium encapsulated into $C_{10}H_{16}$ adamantane, He@adam, is one such example in which the presence or absence of He–C chemical bonds was justified by several leading scientists based on their personal understanding and views to the definition of chemical bond.[92–99] While the presence of four gradient paths connecting He and carbon atoms and the associated values of descriptors like electron density $\rho(r_c)$, Laplacian of electron density $\nabla^2\rho(r_c)$, and energy density $H(r_c)$ at the "bond" critical points of He–C gradient paths lying in between closed-shell and electron-sharing interactions advocate for the presence of chemical bond,[94] the repulsive nature of He–$C_{10}H_{16}$ interaction (154.2 kcal mol^{-1}) contradicts the notion of the presence of chemical bond (see Fig. 6 for the molecular graph).[91,95,97] However, note that the 1997 IUPAC definition of the chemical bond,[100] "there is a chemical bond between two atoms or groups of atoms in the case that the forces acting between them are such as to lead to the formation of aggregation with sufficient stability to make it convenient for the chemist to consider it as

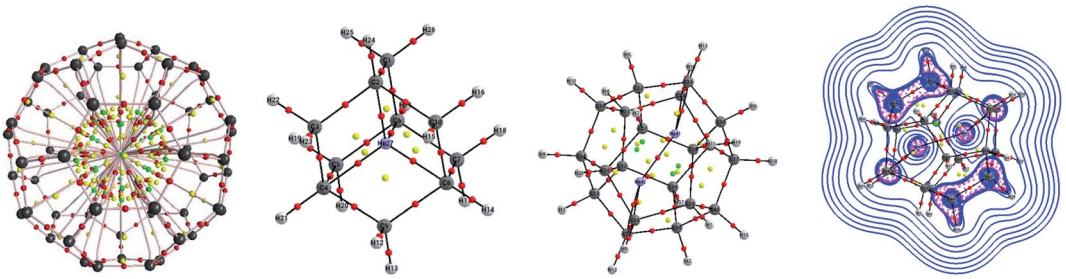

Fig. 6 Molecular graph of Ne@C_{60}, He@adam, and He_2@$C_{20}H_{20}$. The plot of the Laplacian of electron density for the latter complex is also given. Spheres in red, yellow, and green are the bond, ring, and cage critical points.

an independent molecular species", does not demand a chemical bond to be attractive in nature. Bader and co-workers[94] even argued that the interaction between He and carbon atoms connected through the gradient path is attractive in nature. The higher energies of the other carbon and hydrogen atoms are responsible for the energetic instability of the complex against dissociation. Adopting three highly symmetric systems of varying sizes, He@C_8H_8 (O_h), He@$C_{20}H_{20}$ (I_h) and Ng@C_{60} (I_h), Cerpa *et al.*[98] demonstrated that irrelevant to the related Ng–C distances, there always exist gradient paths between them, which are driven by the symmetry, even if the presence of any true chemical bond is very unlikely (see Fig. 6). This is obvious that such conflicting views arise from different perspectives, which are valid within their scope of the definition. Schwarz and co-workers[99] finally proposed that the conflicts may be avoided if such contacts are understood in the light of "confinement bonding".

The presence of the chemical bond in Ng_2@C_{60} involves fewer disputes than the above example. In 2007, Krapp *et al.*[93] made an extensive study on the bonding situation in Ng_2@C_{60} (Ng = He–Xe) complex. Interestingly, upon encapsulation, the Ng–Ng bond lengths get contracted to the 56–68% of the distance in free Ng_2 dimer. Inspection of the energy of HOMO and LUMO of free Ng with those in confined Ng_2 indicates a significant elevation of energy upon confinement, particularly for Ng = Ar–Xe, suggesting that the Ng atoms in the confined state would have different reactivity than that in the free state. The charge distribution indicates that the Ng_2@C_{60} is low for Ng = He–Kr, but remarkably more than one electron is transferred from Xe_2 to the host moiety, making it a charge complex Xe_2^+@C_{60}^-. Importantly, $H(r_c)$ value is considerably negative −0.341 Hartree Å^{-3} for Xe–Xe bond in Xe_2@C_{60}, undoubtedly assigning it as a genuine chemical covalent bond. On the other hand, for Kr–Kr and Ar–Ar, the $H(r_c)$ values are still negative, although they are smaller than that in Xe–Xe. Moreover, the reactivity of Ng_2@C_{60} (Ng = Ar–Xe) would be considerably different than those of free Ng and C_{60}, which was further confirmed by a subsequent study carried out by Solà and co-workers,[101] where they noticed dramatic alteration of reactivity of Ng_2@C_{60} with respect to C_{60} towards Diels–Alder cycloaddition in case of Ng = Ar–Xe. Therefore, it satisfies the IUPAC definition of the chemical bond. Their analyses also categorized the lighter He_2@C_{60} and Ne_2@C_{60} as weakly bonded van der Waals complexes.

It is obvious that the C_{60} cavity is large enough to induce the formation of a chemical bond between two lightest Ng atoms. In order to check whether the bonding situation in He_2 gets changed in case of reasonably smaller host moiety than C_{60}, Cerpa *et al.*[102] forced two He atoms to stay within $C_{20}H_{20}$ cavitand. As expected, such confinement in very small space further squeezes the He–He bond length (1.265 Å), which becomes 0.688 and 1.712 Å shorter than those in He_2@C_{60} and free He_2, respectively. Such He_2 confinement in a small cavity needs to pay a heavy price. The resulting complex is found to be unstable by 169.8 kcal mol^{-1} at the DFT level with respect to the dissociation into free He atoms and $C_{20}H_{20}$. Except for the presence of gradient path between two He atoms, the other bonding indices do not support the presence of chemical bond, which led the authors to conclude that short He–He internuclear separation is a consequence of He-cage repulsion and that it cannot be inferred as a true chemical bond.

To shed light on the difference in Ng–C interaction between the cavity consisting of sp^3 carbons and sp^2 carbons, we performed an energy decomposition analysis combined with natural orbital for chemical valence (EDA-NOCV)[103,104] on Xe_2@C_{60} and He_2@$C_{20}H_{20}$ complexes. Note that because of the different cavity sizes, a comparison between the same Ng atom cannot be done as obviously the orbital interaction in He_2@C_{60} would be minimal. Here, we only emphasize how the most dominating orbital interaction arises in these two cases. Fig. 7 displays the deformation densities and the associated fragment orbitals of these two complexes. In the plot, the electron density flows from the red to blue region. In the case of Xe_2@C_{60}, −63.5 kcal mol^{-1} orbital stabilization arises because of almost one-electron transfer from the antibonding HOMO of Xe_2 to LUMO of C_{60}. Note that this transfer reduces the electron population of antibonding orbital, imposing net bond order in Xe–Xe bond. On the other hand, in the case of He_2@$C_{20}H_{20}$, surprisingly, in place of $1\sigma_u$ orbital, higher-lying $2\sigma_u$ orbital acts as a donor to the LUMO+2 of $C_{20}H_{20}$. It seems that in the confined states, the energy gap between $1\sigma_u$ and $2\sigma_u$ orbitals lowers, introducing some degree of hybridization between them and some electrons from the former orbital polarizes to the latter one. Because of larger spatial distribution than the $1\sigma_u$, $2\sigma_u$ orbital can interact more effectively with LUMO+2 of $C_{20}H_{20}$. However, the degree of such electron transfer and the

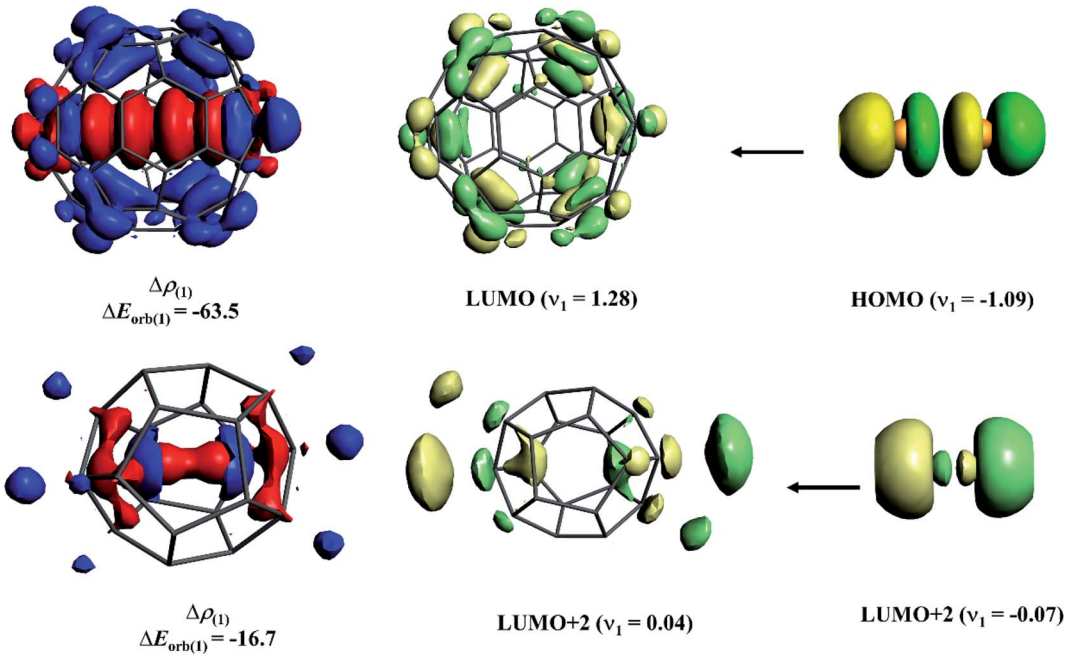

Fig. 7 Shape of the most important deformation density, $\Delta\rho_{(1)}$ of $Xe_2@C_{60}$ and $He_2@C_{20}H_{20}$ corresponding to $\Delta E_{orb(1)}$ in kcal mol^{-1} and the associated fragment orbitals at the BP86-D3(BJ)-ZORA/TZ2P level. The eigenvalues ν_n give the size of the charge migration in e. The direction of the charge flow of the deformation densities is red → blue.

associated orbital interaction is lower than those in $Xe_2@C_{60}$. Such low electron depletion from antibonding orbital corroborates with the previous study[102] where the He–He bond could not be categorized as a chemical bond.

This came as a surprise when Nikolaienko *et al.*[105] argued about the formation of a true He–He bond even in $He_2@C_{60}$ based on Löwdin's postulate. They analytically estimated the potential energy curve of the He–He dimer confined in C_{60} and then perturbatively solved the corresponding Schrödinger equation where they obtained at least one bound state where two He atoms are bound with each other. The *ab initio* MD study on $Ng_2@C_{60}$ showed that Ng_2 units, including He_2, undergo translational, vibrational, and rotational movements as a single entity, without any random movement, supporting some sort of bonding between two He atoms.[57] A similar situation was noted in Ng_2 confined in a smaller cavity like $B_{12}N_{12}$, $B_{16}N_{16}$, and B_{40} cages[106,107] where some specific descriptors support bonding and some criteria do not. Therefore, it is only a matter of weightage an individual wants to give. Some scientists give more weightage on those descriptors that support the formation of chemical bonding, but some others prefer the other way. Nevertheless, it is fun to understand the advantages and limitations of different bonding models in analysing the chemical bonds formed under such drastic conditions. This is important to enjoy the different flavors and opportunities that confinement can provide.

Chemical reactivity of endohedral fullerenes containing Ng atoms

How significant is the effect on the fullerene reactivity due to the encapsulation of an Ng atom? The Diels–Alder reactions were used as a model to address this question both experimentally and theoretically. Saunders and co-workers[108] compared the reactivity of a Diels–Alder reaction between $He@C_{60}$ and $Xe@C_{60}$ with 9,10-dimethylanthracene (DMA) using ^{129}Xe and ^{3}He NMR (Fig. 8a) and found that the equilibrium constant is temperature-dependent. At low temperatures, $He@C_{60}$ is more reactive than $Xe@C_{60}$, while at high temperatures, the opposite occurs. So, the decreased reactivity of $Xe@C_{60}$ towards DMA at low temperatures is because the Xe atom pushes the π-electron cloud of C_{60} outward.

Solà and co-workers[101,109] performed DFT computations to determine the reaction and activation energies for the [4+2] Diels–Alder cycloaddition reactions between $Ng@C_{60}$ or

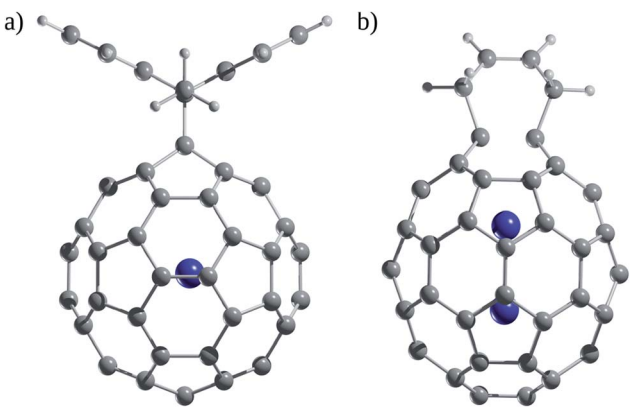

Fig. 8 (a) Diels–Alder adducts between $He@C_{60}$ and $Xe@C_{60}$ with 9,10-dimethylanthracene (DMA). (b) Diels–Alder adducts between $Ng@C_{60}$ and $Ng_2@C_{60}$ (Ng = He–Xe) with 1,3-*cis*-butadiene.

$Ng_2@C_{60}$ (Ng = He–Xe) systems and 1,3-*cis*-butadiene (Fig. 8b). For the free C_{60}, the reaction energies are −20.7 and −4.6 kcal mol^{-1} and activation barriers are 12.7 and 21.0 kcal mol^{-1} for the addition to the [6,6] and [5,6] bonds, respectively. In the case of the $Ng@C_{60}$ systems, the reaction energies (−20.5, −20.3, −20.2, −20.3, and −20.5 kcal mol^{-1} from He to Xe) and barriers (13.0, 13.4, 13.3, 13.1, and 12.9 kcal mol^{-1} from He to Xe) for the addition to the [6,6] bond are quite similar compared to free C_{60}. The same is exhibited by the [5,5] bond with reaction energies of −4.1, −3.9, −3.7, −3.9, and −4.1 kcal mol^{-1} from He to Xe. However, the situation changes for the $Ng_2@C_{60}$ family, the reaction becomes more exothermic going from He_2 to Xe_2 at the most favorable [6,6] bond (−20.9, −23.1, −32.2, −39.9, and −44.9 kcal mol^{-1}) and [5,6] bond (−5.0, −6.4, −15.9, −24.7, and −45.5 kcal mol^{-1}). For the activation barriers, they get decreased as the size of the Ng increases for both most favorable [6,6] bond (12.8, 11.8, 8.4, 6.1, and 3.8 kcal mol^{-1}) and [5,6] bond (20.4, 20.0, 14.9, 11.9, and 5.6 kcal mol^{-1}). In the case of the $Ng@C_{60}$ family, the effect of encapsulation is almost negligible. As expected, the pyracylenic bonds are more reactive than the corannulenic ones. Also, the increased reactivity of the heaviest Ng in the $Ng_2@C_{60}$ family was rationalized in terms of lowering the LUMO energy, a more straining C_{60} cage, and the release of compression of the Ng_2 in the product.

The chemical reactivity of encapsulated Ng atoms was also assessed using chemical descriptors such as the chemical potentials, hardness, electron-donating, and electron-accepting powers. Garza and co-workers[110] used a spherical shell with an attractive potential to simulate the $Ng@C_{60}$ (Ng = He–Kr) systems. All the chemical descriptors were obtained using a DPW92 functional, including a self-interaction correction. The authors concluded that the confinement of Ng atoms increases their chemical potential and electrophilicity, while there is a reduction in the hardness, suggesting a general increment of the reactivity.

Bil *et al.* reported other approaches to assess the influence of Ng (Ng = He–Rn) on the reactivity of fullerenes.[111] They showed, using *ab initio* molecular orbital and MD simulations, that the presence of the endohedral atom influences the ozone ring-opening reaction in $Ng@C_{70}O_3$, but there is almost no effect on the relative stability of the $C_{70}O_3$ isomers by including Ng atoms. The authors also noted that the enthalpy of reaction depends on the isomer considered. For instance, in the case of the *c*,*c*-$C_{70}O_3$ isomer, the reaction profile is not affected by the encapsulated Ng, whereas for *a*,*b*-$C_{70}O_3$ isomer, the enthalpy of reaction increases and for *e*,*e*-$C_{70}O_3$ decreases with the heaviest Ng atoms.

Fernández *et al.*[112] analysed the governing factors for the enhanced reactivity of the Diels–Alder cycloaddition reaction between $Ng_2@C_{60}$ (Ng = He–Xe) and 1,3-butadiene using the activation strain model in combination with the energy decomposition analysis. In the case of $He_2@C_{60}$, the reaction energy (−31.8 kcal mol^{-1}) and the activation energy (13.3 kcal mol^{-1}) are comparable to free C_{60} (−32.1 and 12.7 kcal mol^{-1}, respectively). A stronger effect on the kinetics and thermodynamics is shown for the heavier encapsulated Ng atoms compared to the empty one. The reaction energies are −33.6, −43.1, −51.2, and −56.4 kcal mol^{-1} and the activation energies are 12.4, 9.7, 7.5, and 6.9, respectively, along Ne–Xe. From the analysis of a complete activation strain diagram along the C–C forming bond distance, it is apparent that the stabilizing interaction between the reactants is mainly responsible for the lower computed barriers. The energy decomposition analysis supports that the electrostatic interactions (40–42%) and orbital interactions (43–47%) contribute almost equally to the total interaction energy where the latter term arises as a result of a strong orbital interaction between the cage and the diene induced by a change in the electronic structure of the cage due to the presence of an Ng atom. Thus, the insertion of an Ng dimer leads to remarkably enhanced interaction between the deformed reactant along the reaction coordinate.

Last but not the least questions

What is the smallest carbon fullerene able to confine an Ng? From DFT computations, Sure *et al.*[86] investigated the smallest fullerene skeleton that can encapsulate Ng = He, Ne, Ar atoms in an energetically favorable way. They considered $Ng@C_{20+2n}$ (n = 0, 2–20; Ng = He, Ne, Ar) endohedral fullerenes. Although even $Ng@C_{20}$ complexes are minima on the potential energy surface, a larger space is required to minimize the repulsion. Only attractive interaction (including zero-point energy correction) between Ng and fullerene is noted for the $He@C_{50}$, $Ne@C_{52}$, and $Ar@C_{58}$ complexes. Through their two different sets of DFT computations (PBE/def2-TZVPP and PBE-D3/def2-TZVPP), the authors also justified the essence of taking care of dispersion interaction into the computations to get reliable energetics. Therefore, an Ng endohedral fullerene as small as $Ng@C_{20}$ can be kinetically stable up to a certain extent, but enough large space (C_{50} or larger cage) is required to make it energetically stable. However, up to date only those with $n \geq 60$ have been reported experimentally.

What is the maximum number of Ng atoms contained into a fullerene? Although evidence of more than one Ng atom encapsulated in fullerenes was already known, Tonner *et al.*[88] were the first to address the question using quantum chemical computations. C_{60} is able to fit a maximum of 40He, 17Ne, 7Ar, 6Kr, or 6Xe atoms. Interestingly, there is a quadratic dependence for the dissociation energy with increasing the cluster size and for the volume of the C_{60} cage with an increasing number of endohedral atoms. The decomposition of the dissociation energy into three terms, *viz.*, the compression of the Ng_n cluster, the deformation of the C_{60} cage, and the repulsive interaction between the Ng_n cluster and the C_{60} cage, the last term is mainly responsible for the increased instability along the gradual cluster growth. The same question was considered for the bigger C_{80} cage, where the maximum number of encapsulated Ng atoms increases up to 46He, 24Ne, or 10Ar atoms.[113] Cage opening mechanisms were also reported for C_{80} encapsulating up to or more than 50He, 25Ne, or 12Ar atoms *via* a "molecular cart-type" structure. In both cases, C_{60} and C_{80} are very strong cages with outstanding resistance to high internal pressures.

Can the encapsulation of Ng atoms in a fullerene stabilize other isomers? Merino and co-workers[114] studied the stability of defected fullerenes by encapsulating two Ng atoms inside C_{60}. In fullerenes, the isomers with an isolated pentagon surrounded by hexagons are more stable than those with two pentagons sharing an edge since it prevents the formation of antiaromatic pentalene units (Isolated-Pentagon Rule, IPR). When Xe_2 is confined in C_{60}, the most energetically stable isomer (by 7.0 kcal mol^{-1}) does not follow IPR,[115] rather it has a Stone–Wales defect. The energy decomposition analysis shows that the stability of the $Xe_2@C_{60}$ fullerene with a Stone–Wales defect comes from a lower orbital and electrostatic contributions by 39.4 and 24.5 kcal mol^{-1} (relative to the IPR one) and a decreased steric repulsion between the endohedral Ng dimer and the C_{60} cage due to the ellipsoid shape in the defected fullerene.

Final remarks

Since the discovery of endohedral fullerenes containing Ng atoms in the early 1990s through mass spectroscopy experiments, substantial experimental and theoretical research has been conducted. Over time, various techniques have been developed for the formation of these endohedral fullerenes under extreme conditions (high temperature or pressure) or by molecular surgery. To date, fullerenes containing one or two Ng atoms have been reported. These systems have particular attraction because the guest atoms are, in principle, considered to be inert. However, spectroscopic experiments and quantum computations have proved changes in the properties, bonding, and reactivity of these species. Therefore, derived from the effects induced by confined Ng atoms, the magnetic behavior of the C_{60} or C_{70} cages, bonding, the reactivity of C_{60} to Diels–Alder cycloaddition reactions, and associated kinetics and thermodynamics, along with other electronic properties have been detailedly assessed. MD simulations and quantum chemical computations have been used to model the mechanism of formation/release of endohedral fullerenes, encapsulated with Ng atoms. In addition, the electronic structure and the predominant interactions between encapsulated Ng atoms and fullerene cages along with the reported factors that determine the energy profile for Diels–Alder cycloaddition reactions have been addressed. In general, more pronounced effects are achieved when heavier Ng atoms or a pair of them are encapsulated, such as an enhanced reactivity for the latter case. The future scope of this field is enormous. In place of bare cavitand, it would be interesting to insert Ng atoms in metallofullerenes and to check the resulting energetics and reactivity. The effect of the external electric field on the interaction and bonding in inclusion complexes is another unattained topic. Efforts should also be made about how the stability of Ng encapsulated complexes can be enhanced through doping the fullerenes. Thus, the endohedral fullerenes containing Ng atoms have shown more interesting chemistry than expected.

Conflicts of interest

There are no conflicts to declare.

Acknowledgements

SJ thanks Conacyt for his PhD and Postdoctoral scholarships. JA thanks Conacyt for her PhD scholarships. SP thanks Deutsche Forschungsgemeinschaft for his postdoctoral fellowship.

References

1 H. W. Kroto, J. R. Heath, S. C. O'Brien, R. F. Curl and R. E. Smalley, *Nature*, 1985, **318**, 162–163.
2 H. Sprang, A. Mahlkow and E. E. B. Campbell, *Chem. Phys. Lett.*, 1994, **227**, 91–97.
3 J. R. Heath, S. C. O'Brien, Q. Zhang, Y. Liu, R. F. Curl, F. K. Tittel and R. E. Smalley, *J. Am. Chem. Soc.*, 1985, **107**, 7779–7780.
4 Y. Chai, T. Guo, C. Jin, R. E. Haufler, L. P. Felipe Chibante, J. Fure, L. Wang, J. Michael Alford and R. E. Smalley, *J. Phys. Chem.*, 1991, **95**, 7564–7568.
5 A. A. Popov, S. Yang and L. Dunsch, *Chem. Rev.*, 2013, **113**, 5989–6113.
6 H. Shinohara, *Rep. Prog. Phys.*, 2000, **63**, 843–892.
7 M. N. Chaur, F. Melin, A. L. Ortiz and L. Echegoyen, *Angew. Chem., Int. Ed.*, 2009, **48**, 7514–7538.
8 D. S. Bethune, R. D. Johnson, J. R. Salem, M. S. de Vries and C. S. Yannoni, *Nature*, 1993, **366**, 123–128.
9 T. Weiske, D. K. Böhme, J. Hrušák, W. Krätschmer and H. Schwarz, *Angew. Chem., Int. Ed.*, 1991, **30**, 884–886.
10 T. Weiske, J. Hrušák, D. K. Böhme and H. Schwarz, *Chem. Phys. Lett.*, 1991, **186**, 459–462.
11 T. Weiske, T. Wong, W. Krätschmer, J. K. Terlouw and H. Schwarz, *Angew. Chem., Int. Ed.*, 1992, **31**, 183–185.
12 T. Weiske, D. K. Böhme and H. Schwarz, *J. Phys. Chem.*, 1991, **95**, 8451–8452.
13 M. M. Ross and J. H. Callahan, *J. Phys. Chem.*, 1991, **95**, 5720–5723.
14 T. Weiske, J. Hrušák, D. K. Bohme and H. Schwarz, *Helv. Chim. Acta*, 1992, **75**, 79–89.
15 T. Wong, J. K. Terlouw, T. Weiske and H. Schwarz, *Int. J. Mass Spectrom. Ion Processes*, 1992, **113**, R23–R29.
16 E. E. B. Campbell, R. Ehlich, A. Hielscher, J. M. A. Frazao and I. V. Hertel, *Z. Phys. D: At., Mol. Clusters*, 1992, **23**, 1–2.
17 R. C. Mowrey, M. M. Ross and J. H. Callahan, *J. Phys. Chem.*, 1992, **96**, 4755–4761.
18 Z. Wan, J. F. Christian and S. L. Anderson, *J. Chem. Phys.*, 1992, **96**, 3344–3347.
19 J. Hrušák, D. K. Böhme, T. Weiske and H. Schwarz, *Chem. Phys. Lett.*, 1992, **193**, 97–100.
20 J. F. Christian, Z. Wan and S. L. Anderson, *J. Chem. Phys.*, 1993, **99**, 3468–3479.
21 R. Kleiser, H. Sprang, S. Furrer and E. E. B. Campbell, *Z. Phys. D: At., Mol. Clusters*, 1993, **28**, 89–90.
22 M. Saunders, H. A. Jimenez-Vazquez, R. J. Cross and R. J. Poreda, *Science*, 1993, **259**, 1428–1430.
23 M. Saunders, H. A. Jimenez-Vazquez, R. James Cross, S. Mroczkowski, M. L. Gross, D. E. Giblin and R. J. Poreda, *J. Am. Chem. Soc.*, 1994, **116**, 2193–2194.

24 R. Shimshi, R. J. Cross and M. Saunders, *J. Am. Chem. Soc.*, 1997, **119**, 1163–1164.
25 R.-F. Peng, S.-J. Chu, Y.-M. Huang, H.-J. Yu, T.-S. Wang, B. Jin, Y.-B. Fu and C.-R. Wang, *J. Mater. Chem.*, 2009, **19**, 3602.
26 M. Murata, Y. Murata and K. Komatsu, *Chem. Commun.*, 2008, 6083.
27 Y. Morinaka, F. Tanabe, M. Murata, Y. Murata and K. Komatsu, *Chem. Commun.*, 2010, **46**, 4532–4534.
28 M. Saunders, R. James Cross, H. A. Jiménez Vázquez, R. Shimshi and A. Khong, *Science*, 1996, **271**, 1693–1697.
29 M. Saunders, H. A. Jiménez-Vázquez, R. James Cross, S. Mroczkowski, D. I. Freedberg and F. A. L. Anet, *Nature*, 1994, **367**, 256–258.
30 T. Sternfeld, R. E. Hoffman, M. Saunders, R. J. Cross, M. S. Syamala and M. Rabinovitz, *J. Am. Chem. Soc.*, 2002, **124**, 8786–8787.
31 J. Camacho Gonzalez and A. Muñoz-Castro, *J. Mol. Model.*, 2019, **25**, 322.
32 N. D. Charistos and A. Muñoz-Castro, *J. Phys. Chem. C*, 2018, **122**, 9688–9698.
33 P. R. Birkett, M. Bühl, A. Khong, M. Saunders and R. Taylor, *J. Chem. Soc., Perkin Trans. 2*, 1999, 2037–2039.
34 M. Rüttimann, R. F. Haldimann, L. Isaacs, F. Diederich, A. Khong, H. Jiménez-Vázquez, R. J. Cross and M. Saunders, *Chem.–Eur. J.*, 1997, **3**, 1071–1076.
35 A. Takeda, Y. Yokoyama, S. Ito, T. Miyazaki, H. Shimotani, K. Yakigaya, T. Kakiuchi, H. Sawa, H. Takagi, K. Kitazawa and N. Dragoe, *Chem. Commun.*, 2006, 912–914.
36 K. Yamamoto, M. Saunders, A. Khong, R. James Cross, M. Grayson, M. L. Gross, A. F. Benedetto and R. Bruce Weisman, *J. Am. Chem. Soc.*, 1999, **121**, 1591–1596.
37 M. S. Syamala, R. James Cross and M. Saunders, *J. Am. Chem. Soc.*, 2002, **124**, 6216–6219.
38 Y. Morinaka, S. Sato, A. Wakamiya, H. Nikawa, N. Mizorogi, F. Tanabe, M. Murata, K. Komatsu, K. Furukawa, T. Kato, S. Nagase, T. Akasaka and Y. Murata, *Nat. Commun.*, 2013, **4**, 1554.
39 S. Ito, A. Takeda, T. Miyazaki, Y. Yokoyama, M. Saunders, R. J. Cross, H. Takagi, P. Berthet and N. Dragoe, *J. Phys. Chem. B*, 2004, **108**, 3191–3195.
40 H. M. Lee, M. M. Olmstead, T. Suetsuna, H. Shimotani, N. Dragoe, R. J. Cross, K. Kitazawa and A. L. Balch, *Chem. Commun.*, 2002, 1352–1353.
41 N. Dragoe, A. M. Flank, P. Lagarde, S. Ito, H. Shimotani and H. Takagi, *Phys. Rev. B: Condens. Matter Mater. Phys.*, 2011, **84**, 155448.
42 S. Patchkovskii and W. Thiel, *J. Am. Chem. Soc.*, 1996, **118**, 7164–7172.
43 D. Zahn, *J. Chem. Phys.*, 2005, **123**, 044104.
44 R. Granot and R. Baer, *J. Chem. Phys.*, 2008, **129**, 214102.
45 R. Shimshi, A. Khong, H. A. Jiménez-Vázquez, R. J. Cross and M. Saunders, *Tetrahedron*, 1996, **52**, 5143–5148.
46 T. Ohtsuki, K. Ohno, K. Shiga, Y. Kawazoe, Y. Maruyama and K. Masumoto, *Phys. Rev. Lett.*, 1998, **81**, 967–970.
47 R. J. Cross, A. Khong and M. Saunders, *J. Org. Chem.*, 2003, **68**, 8281–8283.
48 F. Z. Cui, D. X. Liao and H. D. Li, *Phys. Lett. A*, 1994, **195**, 156–162.
49 Z. Xu and J. Yan, *Int. J. Quantum Chem.*, 1995, **53**, 287–295.
50 D. Zahn and G. Seifert, *J. Phys. Chem. B*, 2004, **108**, 16495–16498.
51 S. Patchkovskii and W. Thiel, *Helv. Chim. Acta*, 1997, **80**, 495–509.
52 W. Even, J. Smith and M. W. Roth, *Mol. Simul.*, 2005, **31**, 207–213.
53 M. K. Balasubramanya, M. W. Roth, P. D. Tilton and B. A. Suchy, *J. Comput. Theor. Nanosci.*, 2008, **5**, 627–634.
54 P. Tilton, B. Suchy, M. K. Balasubramanya and M. W. Roth, *Mol. Simul.*, 2007, **33**, 945–952.
55 J.-Y. Li, L.-M. Liu, B. Jin, H. Liang, H.-J. Yu, H.-C. Zhang, S.-J. Chu and R.-F. Peng, *J. Mol. Model.*, 2013, **19**, 1705–1710.
56 B. Cao, T. Peres, R. James Cross, M. Saunders and C. Lifshitz, *J. Phys. Chem. A*, 2005, **109**, 10257–10263.
57 M. Khatua, S. Pan and P. K. Chattaraj, *Chem. Phys. Lett.*, 2014, **610–611**, 351–356.
58 S. Gómez and A. Restrepo, *Phys. Chem. Chem. Phys.*, 2019, **21**, 15815–15822.
59 S. Pan, G. Jana, G. Merino and P. K. Chattaraj, *ChemistryOpen*, 2019, **8**, 173–187.
60 G. Frenking, W. Koch, J. Gauss and D. Cremer, *J. Am. Chem. Soc.*, 1988, **110**, 8007–8016.
61 C. A. Thompson and L. Andrews, *J. Am. Chem. Soc.*, 1994, **116**, 423–424.
62 S. Pan, D. Moreno, J. L. Cabellos, J. Romero, A. Reyes, G. Merino and P. K. Chattaraj, *J. Phys. Chem. A*, 2014, **118**, 487–494.
63 R. Saha, S. Pan, G. Merino and P. K. Chattaraj, *J. Phys. Chem. A*, 2015, **119**, 6746–6752.
64 L. Khriachtchev, M. Räsänen and R. Benny Gerber, *Acc. Chem. Res.*, 2009, **42**, 183–191.
65 R. B. Darzynkiewicz and G. E. Scuseria, *J. Phys. Chem. A*, 1998, **102**, 3458.
66 R. Q. Zhang, W. Y. Ma, K. L. Han and C. S. Lee, *Theor. Chem. Acc.*, 2003, **109**, 278–283.
67 N. N. Breslavskaya, A. A. Levin and A. L. Buchachenko, *Russ. Chem. Bull.*, 2004, **53**, 18–23.
68 N. N. Breslavskaya and A. L. Buchachenko, *Fullerenes, Nanotubes, Carbon Nanostruct.*, 2005, **12**, 47–52.
69 C. N. Ramachandran, D. Roy and N. Sathyamurthy, *Chem. Phys. Lett.*, 2008, **461**, 87–92.
70 A. Hesselmann and T. Korona, *Phys. Chem. Chem. Phys.*, 2011, **13**, 732–743.
71 Y. Ma, Y. Ai, X. Song, C. Wang and Y. Luo, *Chem. Phys. Lett.*, 2014, **591**, 312–316.
72 M. Kolb and W. Thiel, *J. Comput. Chem.*, 1993, **14**, 37–44.
73 A. J. C. Varandas, *Int. J. Quantum Chem.*, 2011, **111**, 416–429.
74 M.-S. Son and Y. K. Sung, *Chem. Phys. Lett.*, 1995, **245**, 113–118.
75 H. A. Jiménez-Vázquez and R. J. Cross, *J. Chem. Phys.*, 1996, **104**, 5589–5593.
76 S. Patchkovskii and W. Thiel, *J. Chem. Phys.*, 1997, **106**, 1796–1799.

77 M. Bühl, S. Patchkovskii and W. Thiel, *Chem. Phys. Lett.*, 1997, **275**, 14–18.
78 L. Pang and F. Brisse, *J. Phys. Chem.*, 1993, **97**, 8562–8563.
79 A. D. Becke, *Phys. Rev. A*, 1988, **38**, 3098–3100.
80 C. Lee, W. Yang and R. G. Parr, *Phys. Rev. B: Condens. Matter Mater. Phys.*, 1988, **37**, 785–789.
81 J. P. Perdew, *Phys. Rev. B: Condens. Matter Mater. Phys.*, 1986, **33**, 8822–8824.
82 A. D. Becke, *J. Chem. Phys.*, 1993, **98**, 5648–5652.
83 I. D. Mackie and G. A. DiLabio, *J. Phys. Chem. A*, 2008, **112**, 10968–10976.
84 S. Grimme, *J. Comput. Chem.*, 2006, **27**, 1787–1799.
85 Y. Zhao and D. G. Truhlar, *Theor. Chem. Acc.*, 2008, **120**, 215–241.
86 R. Sure, R. Tonner and P. Schwerdtfeger, *J. Comput. Chem.*, 2015, **36**, 88–96.
87 S. Grimme, J. Antony, S. Ehrlich and H. Krieg, *J. Chem. Phys.*, 2010, **132**, 154104.
88 R. Tonner, G. Frenking, M. Lein and P. Schwerdtfeger, *ChemPhysChem*, 2011, **12**, 2081–2084.
89 J. Camacho Gonzalez, S. Mondal, F. Ocayo, R. Guajardo-Maturana and A. Muñoz-Castro, *Int. J. Quantum Chem.*, 2020, **120**, 119.
90 J. Autschbach and E. Zurek, *J. Phys. Chem. A*, 2003, **107**, 4967–4972.
91 P. Pyykkö, C. Wang, M. Straka and J. Vaara, *Phys. Chem. Chem. Phys.*, 2007, **9**, 2954–2958.
92 A. Haaland, D. J. Shorokhov and N. V. Tverdova, *Chem.–Eur. J.*, 2004, **10**, 4416–4421.
93 A. Krapp and G. Frenking, *Chem.–Eur. J.*, 2007, **13**, 8256–8270.
94 R. F. W. Bader and D.-C. Fang, *J. Chem. Theory Comput.*, 2005, **1**, 403–414.
95 T. Strenalyuk and A. Haaland, *Chem.–Eur. J.*, 2008, **14**, 10223–10226.
96 M. von Hopffgarten and G. Frenking, *Chem.–Eur. J.*, 2008, **14**, 10227–10231.
97 J. Poater, M. Solà and F. M. Bickelhaupt, *Chem.–Eur. J.*, 2006, **12**, 2889–2895.
98 E. Cerpa, A. Krapp, A. Vela and G. Merino, *Chem.–Eur. J.*, 2008, **14**, 10232–10234.
99 S.-G. Wang, Y.-X. Qiu and W. H. Eugen Schwarz, *Chem.–Eur. J.*, 2009, **15**, 6032–6040.
100 A. D. McNaught and A. Wilkinson, *Compendium of Chemical Terminology: IUPAC Recommendations*, Wiley-Blackwell, 1997.
101 S. Osuna, M. Swart and M. Solà, *Chem.–Eur. J.*, 2009, **15**, 13111–13123.
102 E. Cerpa, A. Krapp, R. Flores-Moreno, K. J. Donald and G. Merino, *Chem.–Eur. J.*, 2009, **15**, 1985–1990.
103 T. Ziegler and A. Rauk, *Theor. Chim. Acta*, 1977, **46**, 1–10.
104 M. Mitoraj and A. Michalak, *Organometallics*, 2007, **26**, 6576–6580.
105 T. Yu Nikolaienko, E. S. Kryachko and G. A. Dolgonos, *J. Comput. Chem.*, 2018, **39**, 1090–1102.
106 M. Khatua, S. Pan and P. K. Chattaraj, *J. Chem. Phys.*, 2014, **140**, 164306.
107 S. Pan, M. Ghara, S. Kar, X. Zarate, G. Merino and P. K. Chattaraj, *Phys. Chem. Chem. Phys.*, 2018, **20**, 1953–1963.
108 M. Frunzi, R. J. Cross and M. Saunders, *J. Am. Chem. Soc.*, 2007, **129**, 13343–13346.
109 S. Osuna, M. Swart and M. Solà, *Phys. Chem. Chem. Phys.*, 2011, **13**, 3585–3603.
110 A. Cortés-Santiago, R. Vargas and J. Garza, *J. Mex. Chem. Soc.*, 2017, **56**, 270–274.
111 A. Bil and C. A. Morrison, *J. Phys. Chem. A*, 2012, **116**, 3413–3419.
112 I. Fernández, M. Solà and F. M. Bickelhaupt, *J. Chem. Theory Comput.*, 2014, **10**, 3863–3870.
113 Z. Mahdavifar, *J. Mol. Graphics Modell.*, 2014, **54**, 32–45.
114 S. Jalife, S. Mondal, J. L. Cabellos, S. Pan, M. Á. Méndez-Rojas, I. Fernández, G. Frenking and G. Merino, *ChemistrySelect*, 2016, **1**, 2405–2408.
115 H. W. Kroto, *Nature*, 1987, **329**, 529–531.

